APL Photonics

LETTER | APRIL 02 2025

Entanglement transfer during quantum frequency conversion in gas-filled hollow-core fibers

Tasio Gonzalez-Raya ; Arturo Mena ; Miriam Lazo ; Luca Leggio ; David Novoa ; Mikel Sanz

APL Photonics 10, 041302 (2025)
https://doi.org/10.1063/5.0246782

Entanglement transfer during quantum frequency conversion in gas-filled hollow-core fibers

Cite as: APL Photon. 10, 041302 (2025); doi: 10.1063/5.0246782
Submitted: 4 November 2024 • Accepted: 18 March 2025 •
Published Online: 2 April 2025

Tasio Gonzalez-Raya,[1,2,a)] Arturo Mena,[3] Miriam Lazo,[4] Luca Leggio,[1,3] David Novoa,[2,3,5] and Mikel Sanz[1,2,4,5]

AFFILIATIONS

[1] Basque Center for Applied Mathematics (BCAM), Alameda de Mazarredo 14, 48009 Bilbao, Spain
[2] EHU Quantum Center, University of the Basque Country UPV/EHU, Bilbao, Spain
[3] Department of Communications Engineering, Engineering School of Bilbao, University of the Basque Country UPV/EHU, Torres Quevedo 1, 48013 Bilbao, Spain
[4] Department of Physical Chemistry, University of the Basque Country UPV/EHU, Apartado 644, 48080 Bilbao, Spain
[5] IKERBASQUE, Basque Foundation for Science, Plaza Euskadi 5, 48009 Bilbao, Spain

[a)] **Author to whom correspondence should be addressed:** tgonzalez@bcamath.org

ABSTRACT

Quantum transduction is essential for the future hybrid quantum networks, connecting devices across different spectral ranges. In this regard, molecular modulation in hollow-core fibers has proven to be exceptional for efficient and tunable frequency conversion of arbitrary light fields down to the single-photon limit. However, insights into this conversion method for quantum light have remained elusive beyond standard semi-classical models. In this Letter, we employ a quantum Hamiltonian framework to characterize the behavior of entanglement during molecular modulation while describing the quantum dynamics of both molecules and photons in agreement with recent experiments. In particular, apart from obtaining analytical expressions for the final opto-molecular states, our model predicts a close correlation between the evolution of the average photon numbers and the transfer of entanglement between the interacting parties. These results will contribute to the development of new fiber-based strategies to tackle the challenges associated with the upcoming generation of lightwave quantum technologies.

I. INTRODUCTION

Understanding light–matter interactions at the quantum level lies at the core of the recent developments in quantum technologies[1–4] that are behind sophisticated systems such as the future hybrid quantum networks.[5] These systems comprise multiple devices such as quantum light sources,[6,7] repeaters,[8,9] memories,[10,11] and fiber transmission lines,[12] which operate across different spectral regions of the optical domain, in sharp contrast to, for example, the microwave superconducting circuits employed in state-of-the-art quantum computers.[13,14] Thus, efficient frequency transduction of quantum light states between disparate domains[15–17] is essential to bridge the operational gaps between nodes.[18] This has encouraged the proposal and demonstration of many different strategies to tackle this challenge in different platforms.[19–30] Recently, molecular modulation in hollow-core anti-resonant fibers (ARFs) filled with gas[31,32] has stood out owing to its tunability, large frequency shifts, near-unity efficiency, and exquisite preservation of non-classical correlations.[33–35] This is facilitated by the tight light-matter confinement in the core,[31] ultra-low attenuation over a broad bandwidth[32] and pressure-adjustable optical properties,[36] which make ARFs excellent vehicles for light-based quantum applications.[37,38]

On the other hand, in molecular modulation[39,40] at the single-photon level, a quantum light state scatters off the molecular coherence waves pre-excited via stimulated Raman scattering (SRS) in the ARF core, changing its frequency by the appropriate Raman shift without a threshold. The corresponding state can be controllably up- or down-converted, provided specific phase-matching conditions are fulfilled, which, in the case of gas-filled ARFs, is achieved by leveraging the fiber dispersion.[41,42]

Despite the great potential of ARF-based molecular modulation for quantum transduction,[34] it still remains unclear whether intrinsic quantum properties such as entanglement can be transferred with high fidelity from the original to the target states during the conversion process, a question that cannot be answered using the widely employed Maxwell–Bloch formalism.[43,44] The main reason is its classical treatment of the light fields, although it has been applied to the modeling of certain quantum optical phenomena, like photon absorption and emission in weakly excited atomic clouds.[45] Recent efforts in this direction have provided further insights into the changes in photonic correlations after frequency conversion.[46] Nevertheless, a more detailed description of the internal quantum light-quantum matter interactions down to the single-photon limit has, to our best knowledge, so far not been adapted to molecular modulation-based frequency conversion in ARFs.

In this Letter, we describe both the preparation of the molecular state through SRS, as well as the subsequent thresholdless frequency-conversion process at the single-photon level by employing a quantum Hamiltonian model that allows us to study the behavior of entanglement during molecular modulation. In particular, considering the experimental scenario reported in Ref. 34, we are able to characterize the state of the molecules and predict a complete transfer of entanglement between one of the frequencies of a Bell state and its corresponding frequency-converted counterpart. Our results may aid the design, optimization, and interpretation of future experiments in light-based quantum technologies using ARFs and their subsequent applications.

II. QUANTUM DESCRIPTION OF MOLECULAR MODULATION

A. Preparation of the molecular state

The process we want to describe is molecular modulation assisted by SRS.[47,48] We consider two-level molecules in general and, inspired by recent experiments,[34,35,49,50] we focus on the $Q(1)$ vibrational transition of hydrogen as a good two-level approximation. This transition is dipole-forbidden, and therefore requires a two-photon process, such as Raman scattering, to occur (depicted in Fig. 1). In this process, the pump photons launched in the fundamental core mode of the H_2-filled ARF (illustrated in Fig. 2) are scattered into the Stokes or anti-Stokes frequencies depending on whether they excite or de-excite the molecules, respectively. These transitions are illustrated in Fig. 1, where ω_P, ω_S, and ω_A are the central angular frequencies of the narrowband pump, Stokes, and anti-Stokes signals, respectively, and Ω represents the Raman shift, such that $\omega_S = \omega_P - \Omega$ and $\omega_A = \omega_P + \Omega$. For the H_2 gas case, $\Omega/2\pi \approx 125$ THz,[51] the largest molecular shift in nature. Without loss of generality, the light is linearly polarized in our analysis, and therefore rotational states are highly disfavored. Furthermore, hereafter we will consider all the optical frequencies involved in the dynamics

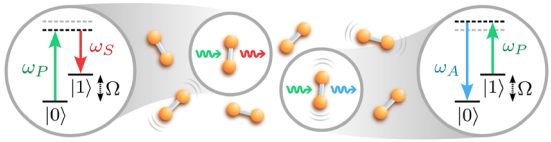

FIG. 1. Illustration of Raman scattering in a molecular diatomic gas. (Left) A photon with pump frequency ω_P is inelastically scattered by a molecule in the vibrational ground state $|0\rangle$. As a result of the interaction, the molecule gains an energy defined by the Raman frequency Ω, transitioning into the excited vibrational state $|1\rangle$. Meanwhile, the scattered photon ends with Stokes frequency $\omega_S = \omega_P - \Omega$. (Right) The inverse process is also represented, involving the de-excitation of molecules via the inelastic scattering of a pump photon into the anti-Stokes frequency $\omega_A = \omega_P + \Omega$. Dashed lines indicate off-resonant energy levels.

contained in the fundamental transmission band of the ARF, that is, spectrally away from loss-inducing resonances with spatial modes localized in the cladding elements.[32]

The quantum Hamiltonian describing the pump, Stokes, and anti-Stokes frequencies of the electric field interacting with a single molecule is expressed as $H = H_0 + V$.[52,53] On one hand, we have the unperturbed part of the Hamiltonian H_0, defined as

$$H_0/\hbar = \omega_0|0\rangle\langle 0| + \omega_1|1\rangle\langle 1| + \sum_{i=2}^{\infty} \omega_i|i\rangle\langle i| + \sum_l \omega_l a_l^\dagger a_l, \tag{1}$$

where $l \in \{P, S, A\}$ labels the operators associated with the pump, Stokes, and anti-Stokes frequencies, respectively, and ω_l are the photonic frequencies. The quantity $\hbar\omega_i$ is the energy associated with the vibrational states $|i\rangle$ of the molecule. On the other hand, the interaction part of the Hamiltonian, V, is given by

$$V = \sum_{i,j}\sum_l g_{i,j}^l |i\rangle\langle j|\left(a_l e^{i\beta_l z} - a_l^\dagger e^{-i\beta_l z}\right), \tag{2}$$

where $g_{i,j}^l$ is the coupling strength between levels $|i\rangle$ and $|j\rangle$ via the bosonic mode l, and β_l is the propagation constant for frequency ω_l. Let us now eliminate the higher energy levels, that is, levels with $i > 1$, to obtain an effective Hamiltonian describing the interaction of the pump, Stokes, and anti-Stokes frequencies, with the molecule. To do this, we go to an interaction picture with respect to H_0 and perform a rotating-wave approximation, keeping only the static terms up to second order in the coupling strength. That is, by assuming that $g_{i,j}^l\sqrt{N_l} \ll \hbar|\omega_i - \omega_j \pm \omega_l|$, with N_l the number of photons with frequency ω_l, we keep only the resonant terms. The relevant resonances in this system are $\omega_P - \omega_S = \Omega = \omega_A - \omega_P$, with $\Omega \equiv \omega_1 - \omega_0$. Extending this approach to a system with N molecules results in the following effective Hamiltonian:[54]

$$\begin{aligned} H_{\text{eff}} = {} & \hbar\Omega J_z + \hbar\sum_l \left(\omega_l + \Delta_l^+\right)a_l^\dagger a_l + 2\hbar\sum_l \Delta_l^- a_l^\dagger a_l J_z \\ & + \hbar\left(G_S e^{i\Delta\beta z} a_P a_S^\dagger + G_A e^{i\Delta\beta' z} a_P^\dagger a_A\right)J^+ \\ & + \hbar\left(G_S^* e^{-i\Delta\beta z} a_P^\dagger a_S + G_A^* e^{-i\Delta\beta' z} a_P a_A^\dagger\right)J^-, \end{aligned} \tag{3}$$

where $G_{S(A)}$ is the interaction strength between pump, (anti-) Stokes, and the molecules, $\Delta_l^\pm$ represent the Stark shifts, and $\Delta\beta \equiv \beta_P - \beta_S$ and $\Delta\beta' \equiv \beta_A - \beta_P$. The global spin operators are defined through

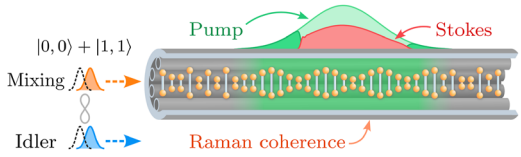

FIG. 2. Schematic representation of the experimental layout considered. A pump beam generates Raman vibrational excitations in the gas molecules, preparing them in a coherent and synchronized vibrational motion. During this process, the pump is depleted into the Stokes frequency, as represented in the figure. The mixing signal simultaneously propagating with the pump perceives the molecular coherence wave and is scattered to a higher frequency. Although the gas molecules are depicted equidistantly along a longitudinal axis for illustrative purposes, they actually fill the whole interior of the fiber and are randomly located and oriented.

the 1/2-spin operators as $J_z = \oplus_{l=1}^{N}\sigma_l^z/2$ and $J^{\pm} = \oplus_{l=1}^{N}\sigma_l^{\pm}$, with $\sigma^z = |1\rangle\langle 1| - |0\rangle\langle 0|$, $\sigma^+ = |1\rangle\langle 0|$, and $\sigma^- = |0\rangle\langle 1|$. They satisfy $[J_z, J^{\pm}] = \pm J^{\pm}$ and $[J^+, J^-] = 2J_z$ and, as operators, they act on global spin states of the form $|\mathbf{N/2}, m_z\rangle$ with $m_z \in \{-N/2, \ldots, N/2\}$. Note that these operators treat the molecular gas as an ensemble of two-level systems and they are *not* representing actual angular momentum of the molecules or light polarization. More details on the derivation of H_{eff} can be found in the supplementary material.

The excitation of molecular coherence manifests itself as a synchronous oscillation of the gaseous core. This is shown in Fig. 2, where the molecules are depicted equidistantly along a longitudinal axis with the same orientation for illustrative purposes, whereas in reality, the gas fills the whole interior of the fiber and the molecules are randomly oriented. In this regard, the interaction will be more significant with the percentage of molecules aligned with the linearly polarized fields, which is already taken into account in the coupling constants obtained phenomenologically (see supplementary material). In Ref. 34, the molecular coherence was generated by a nanosecond pump pulse with an energy of 115 μJ. This means that the initial state of the pump can be considered as a coherent state with $\alpha_P \approx 2.48 \times 10^7$, enabling a few approximations that simplify Eq. (3). First, the annihilation of pump photons leads to the generation of intense laser radiation at the down-shifted Stokes frequency along the fiber length.[55] Therefore, we may consider a semiclassical approximation, replacing the operators in both pump and Stokes frequencies by classical variables $a_P \to \alpha_P$ and $a_S \to \alpha_S$ in Eq. (3). In addition, since the majority of molecules remain in their ground state, the photon population of the anti-Stokes frequency is usually negligible in this process, allowing us to discard it in our analysis. Finally, we consider that the Stark shifts are also negligible, $\Delta_P^{\pm} = \Delta_S^{\pm} \approx 0$. Before performing the semiclassical approximation, in order to avoid oscillations with Ω in the expectation values, we transform the Hamiltonian into an interaction picture with respect to $\Omega J_z + \omega_P a_P^{\dagger} a_P + \omega_S a_S^{\dagger} a_S$, obtaining

$$H_{\alpha}^{I} = \hbar\left(G_S e^{i\Delta\beta z}\alpha_P\alpha_S^* J^+ + G_S^* e^{-i\Delta\beta z}\alpha_P^*\alpha_S J^-\right). \tag{4}$$

By evolving the initial state of the molecules $\left|\frac{\mathbf{N}}{2}, -\frac{N}{2}\right\rangle$, which corresponds to all molecules in the ground state, under this Hamiltonian for a time t, we find the state in the interaction picture:

$$|s\rangle = \left(\frac{e^{-i\Omega t}}{1+|s|^2}\right)^{\frac{N}{2}} \sum_{n=0}^{N}\binom{N}{n}^{1/2} s^n \left|\frac{\mathbf{N}}{\mathbf{2}}, -\frac{N}{2}+n\right\rangle. \tag{5}$$

Here, we have

$$s = -ie^{i\Delta\beta z}\tan\left(G_S\alpha_P\alpha_S t\right), \tag{6}$$

where we have assumed that G_S, α_P, and α_S are real. The supplementary material and Ref. 56 include the mathematical steps to find $|s\rangle$.

The emergence of vibrational coherence in the molecular gas, highlighted in green inside the fiber at Fig. 2, originates from the beating between the pump and Stokes fields.[42,44,57] As the amplitude of the coherence wave rises, the pump starts to suffer depletion and the Stokes starts to be amplified. As the depletion continues, the beating between the fields becomes weaker, preventing the generation of new coherence. Meanwhile, the existing coherence wave fades away due to collisional dephasing on a time scale T_2. However, in a temporal reference frame moving with the co-propagating pump and Stokes pulses at their group velocity, new coherence will be found over a longer time scale as light travels through the fiber, since the amplitude of the coherence wave at a given relative time coordinate is the result of the integrated effects induced by these pulses at previous times.[44] Hence, the excited molecular coherence is harvested, within its lifetime, for frequency conversion of an arbitrary mixing signal. Unlike usual SRS, in which the power of the scattered pump beam needs to be higher than a minimum threshold, this frequency conversion process is thresholdless and, hence, it can be applied to a single photon. In addition, the phase-matching conditions governing the feasibility of frequency conversion of the mixing signal are highly influenced by the dispersion contributions from both the gas and the geometry of the waveguide.[41,42] In a nutshell, if the difference in the propagation constants of the ARF modes at the original and converted photon frequencies matches the propagation constant of the molecular coherence wave (given by the difference between those of the pump and Stokes fields), energy will be efficiently exchanged during the scattering event, resulting in a modification of the photon frequency according to the molecular Raman shift.

B. Mixing frequency conversion

In the following, let us use the developed framework to analyze the frequency conversion process of one of the frequency components of a maximally-entangled Bell state. Indeed, we will convert the mixing frequency by launching it simultaneously with the pump beam, while the idler frequency remains unperturbed outside the fiber, and observe the entanglement dynamics between the idler and the mixing and up-converted frequencies. Considering the conditions of Ref. 34, the experimental system undergoes a phase-matched transition between a mixing frequency of ≈210 THz (1425 nm in wavelength) and an up-converted frequency of ≈335 THz (895 nm). Even though this is not strictly a Raman transition, it can be described using a Hamiltonian with the same structure as in Eq. (3). This time, the terms describing the mixing to up-converted interaction mimic those of the pump to anti-Stokes, but with the appropriate parameters.

While the idler and the mixing fields are initially prepared in a Bell state, the up-converted field is in the vacuum state; therefore, the initial state is simply $(|0,0,0\rangle + |1,1,0\rangle)/\sqrt{2}$. This notation represents, from left to right and separated by commas, the number of photons in the idler, mixing, and up-converted frequencies, respectively. Since in the experiments[34,36,42] we typically have a large number of molecules ($\sim 10^{18}$), the energy state of the molecular ensemble will not change significantly due to the introduction of a single excitation into the system. Thus, in the Hamiltonian characterizing the frequency-conversion process, we replace the global spin operators by their expectation values over the spin coherent state in Eq. (5). That is, we replace $J^+ \to \xi^*$ and $J^- \to \xi$, with

$$\xi = \langle s|J^-|s\rangle = -ie^{i\Delta\beta z}\frac{N}{2}\sin(2G_S\alpha_P\alpha_S t). \tag{7}$$

Before continuing, let us transform the Hamiltonian into an interaction picture again with respect to $\Omega J_z + \omega_M a_M^\dagger a_M + \omega_U a_U^\dagger a_U$, where ω_M and ω_U are the mixing and up-converted angular frequencies. Then, the resulting Hamiltonian is

$$H_\xi^I = \hbar G_U\Big(\xi^* e^{i[(\Omega+\omega_M-\omega_U)t-(\beta_M-\beta_U)z]}a_M^\dagger a_U + \xi e^{-i[(\Omega+\omega_M-\omega_U)t-(\beta_M-\beta_U)z]}a_M a_U^\dagger\Big), \tag{8}$$

where G_U represents the interaction strength between the mixing, the up-converted, and the molecules, and is supposed to be real. If we assume that, as in the experiments, the phase matching and resonance conditions are satisfied, we would have $\beta_U - \beta_M = \Delta\beta \equiv \beta_P - \beta_S$ and $\omega_U - \omega_M = \Omega \equiv \omega_P - \omega_S$, respectively. Note that we do not necessarily require $\omega_l = \omega_m$ or $\beta_l = \beta_m$ with $l \in \{P,S\}$ and $m \in \{M,U\}$ and that, experimentally, these conditions can be adjusted to carry out frequency down-conversion as well, owing to the excellent tunability of gas-filled ARFs.[41,42]

Note that this Hamiltonian is similar to others found in the context of quantum frequency conversion.[58,59] Using these conditions and H_ξ^I to evolve the Bell state considered for the idler and the mixing photons, we obtain a state that, when transformed back to the Schrödinger picture, it becomes

$$|\psi\rangle = \frac{1}{\sqrt{2}}\big(|0,0,0\rangle + \cos(G_U|\xi|t)|1,1,0\rangle + e^{-i\Omega t}\sin(G_U|\xi|t)|1,0,1\rangle\big), \tag{9}$$

which is heavily modulated by the state of the gaseous molecular ensemble via ξ, and is analogous to the ones found in other quantum frequency conversion schemes.[23] Therefore, in this framework, the resulting equations for the evolution of the mixing, NM, and the up-converted, N_U, average photon numbers during molecular modulation are

$$N_M = \frac{1}{2}\cos^2(G_U|\xi|t), \tag{10}$$

$$N_U = \frac{1}{2}\sin^2(G_U|\xi|t). \tag{11}$$

Meanwhile, we also study the dynamics of entanglement between the mixing and the up-converted frequencies through the concurrence,[60] an entanglement monotone used for bipartite mixed states.

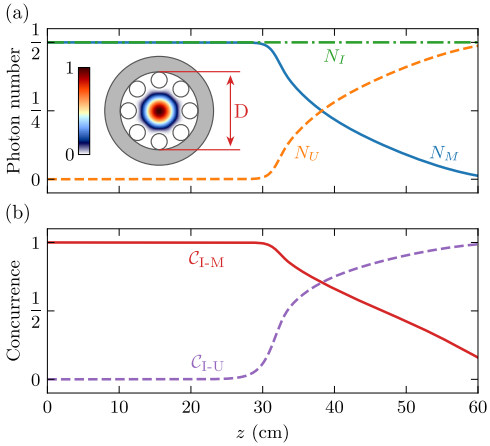

FIG. 3. Evolution of the average photon numbers and concurrences along the fiber filled with 70 bar H_2 and pumped with 115 μJ pulse energy. (a) Average photon numbers of the idler, N_I, mixing, N_M, and up-converted, N_U, frequency modes. The inset shows the simulated transverse intensity distribution (normalized to its maximum) of the fundamental core mode in a single-ring-type ARF similar to that used in Ref. 34 (see Table I in the supplementary material). Here, D represents the larger internal diameter of the fiber. (b) Dynamics of the idler-mixing, $C_{I\text{-}M}$, and idler-up-converted, $C_{I\text{-}U}$, concurrences.

This is an appropriate choice in this case since we have entanglement not only between the idler and the mixing subsystems, but also between the idler and up-converted. Furthermore, the concurrence completely characterizes the entanglement of formation[61] for a pair of two-level systems. In our case, we find that the idler-mixing and the idler-up-converted concurrences are

$$C_{\text{I-M}} = |\cos(G_U|\xi|t)|, \tag{12}$$

$$C_{\text{I-U}} = |\sin(G_U|\xi|t)|. \tag{13}$$

Notice how entanglement transfer between mixing and up-converted modes is closely related to the evolution of the number of photons in each frequency mode, and thus higher conversion efficiencies lead to a more effective entanglement transfer. The time parameter t here is considered to be related to the propagation distance z inside the fiber used in Ref. 34, $z \approx ct$. This is used to represent the evolution of the average photon numbers and the concurrences in Fig. 3, where the explicit time dependence of α_P and α_S, as shown in the supplementary material, has been considered. These coefficients are obtained by numerically solving the semiclassical Maxwell–Bloch equations of motion for the pump and Stokes electric fields.[44,57] These already include the phenomenological T_2 factor accounting for the temporal dephasing of the molecular coherence. In addition, to obtain the coupling strength, we have estimated the quantization volume based on the geometric properties of the waveguide, such as the larger internal diameter D (see Fig. 3) and the temporal length of the interaction.

III. RESULTS

In Fig. 3(a), we show the average photon numbers for the mixing, up-converted, and idler frequencies by blue solid, orange

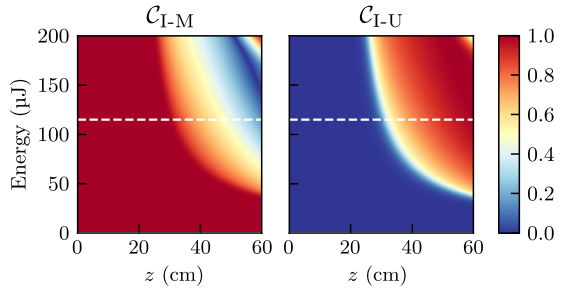

FIG. 4. Concurrence as a function of the initial pump beam energy and the propagation distance **z**. The plots show the evolution of the idler-mixing $C_{I\text{-}M}$ and idler-up-converted $C_{I\text{-}U}$ concurrences at a pressure of 70 bar. The white dashed lines correspond to the evolution displayed in Fig. 3.

dashed, and green dashed-dotted lines, respectively. In Fig. 3(b), we do the same for the idler-mixing and the idler-up-converted concurrences using red solid and purple dashed lines, respectively. We can observe that, until molecular coherence becomes significant at around the middle of the fiber, no substantial conversion dynamics occur; from that point on, the probability of frequency up-converting a mixing photon increases, and this is reflected in higher entanglement between idler and up-converted frequencies. Meanwhile, the idler-mixing concurrence decreases. Furthermore, notice that the crossings between the average photon numbers and the concurrences occur at exactly the same point, around $z \approx 38$ cm, as a consequence of the close relation between the transfer of entanglement and the transfer of photon population. Note that, here, the maximum value for the average photon numbers is 1/2 due to the type of photonic quantum state considered as input to the system. After a quarter of an oscillation, that is, when $G_U|\xi|t = \pi/2$, we find the state $\big(|0,0,0\rangle + e^{-i\Omega t}|1,0,1\rangle\big)/\sqrt{2}$ for the idler, mixing, and up-converted, respectively. This state showcases that high efficiencies in the transfer of a photon from the mixing to the up-converted mode can be theoretically attainable, as can be seen from Eqs. (10) and (11). Note that our predictions could be tested in future experiments, since efforts to characterize the concurrence of mixed states have already been made,[62] obtaining lower[63] and upper bounds[64] of this quantity.

A deeper analysis of the concurrence dynamics is presented in Fig. 4, where the influence of the initial pump pulse energy is clearly shown. In general, the concurrence varies smoothly as the energy parameter is modified, indicating stable dynamics. In addition to this, Fig. 4 indicates that the transfer dynamics can be tuned to be produced at shorter z values by increasing the initial pump pulse energy.

IV. CONCLUSION

In conclusion, we have explored the use of molecular modulation triggered by SRS in gas-filled ARFs for frequency up-conversion of entangled photon pairs, showing how entanglement can be efficiently transferred to the frequency-converted counterpart. To do so, we employ a quantum Hamiltonian description capable of recovering the Maxwell–Bloch equations in the semiclassical limit, as shown in the supplementary material. With it, we were able to characterize the state of the molecules as the vibrational coherence is established and to use it in the analysis of the molecular modulation of quantum light states injected in gas-filled ARFs. We derived simple expressions governing the evolution of entanglement in the system, demonstrating the close relationship with the evolution of the average photon numbers.

We have found the single-mode treatment of both frequency and spatial modes to be satisfactory for the scope of this work, following the conditions of Ref. 34. Nevertheless, a leap into a full multimode theory could be taken, for example, by following the quantum treatment in Ref. 46. This provides a description of the general effects of frequency translation in the shape of the second-order time correlations of the experiment in Ref. 34 by considering the bandwidth in the quantum frequency mode distribution of the initial photonic state. Moreover, one can follow the works in Refs. 65–68, which studied the role of the field bandwidths during the preparation of the Raman molecular coherence in the semiclassical regime. In addition, semiclassical treatments that deal with multiple spatial modes have also been considered[69,70] following the lines of Ref. 44.

As the experiments in this area are rapidly progressing, we believe that this framework will be a useful resource for the design of novel fiber-based quantum transduction strategies that could be fully integrated with existing fiber networks, thereby bringing the dream of future quantum networks one step closer.

SUPPLEMENTARY MATERIAL

In the supplementary material, we provide more detailed calculations on the derivation of H_{eff}, the molecular state, and the concurrences. The experimental parameters used in Ref. 34 and the subsequent time dependence of α_P and α_S can also be found.

ACKNOWLEDGMENTS

We acknowledge financial support from HORIZON-CL4-2022-QUANTUM01-SGA Project No. 101113946 OpenSuperQ-Plus100 of the EU Flagship on Quantum Technologies, the Spanish Ramón y Cajal Grant No. RYC-2020-030503-I, Project Grant Nos. PID2021-125823NA-I00, PID2021-123131NA-I00, PID2021-122505OBC31, and TED2021-129959B-C21, funded by MICIU/AEI/10.13039/501100011033 and by "ERDF A way of making Europe," by "ERDF Invest in your Future," by the "European Union NextGenerationEU/PRTR" and "ESF+," from the Basque Government through Grant Nos. IT1470-22 and IT1455-22 and ELKARTEK (Grant Nos. μ4Smart-KK-2023/00016, Ekohegaz II-KK-2023/00051, and KUBIT KK-2024/00105), and from the IKUR Strategy under the collaboration agreement between the Ikerbasque Foundation and BCAM on behalf of the Department of Education of the Basque Government and Grant No. IKUR_IKA_23/04. ML acknowledges support from the predoctoral grant "Formación de Profesorado Universitario" FPU23/02350 from the Spanish Ministry of Science, Innovation and Universities (MICIU). This work has also been financially supported by the Ministry for Digital Transformation and the Civil Service of the Spanish Government through the QUANTUM ENIA project call – Quantum Spain project, and by the European Union through the Recovery, Transformation and Resilience Plan – NextGenerationEU within the framework of the Digital Spain 2026 Agenda.

AUTHOR DECLARATIONS

Conflict of Interest

The authors have no conflicts to disclose.

Author Contributions

T.G.-R. and A.M. contributed equally to this work.

Tasio Gonzalez-Raya: Formal analysis (equal); Methodology (lead); Software (equal); Writing – original draft (equal). **Arturo Mena**: Formal analysis (equal); Methodology (equal); Software (equal); Visualization (lead); Writing – original draft (equal). **Miriam Lazo**: Methodology (supporting). **Luca Leggio**: Visualization (supporting); Writing – review & editing (equal). **David Novoa**: Conceptualization (equal); Funding acquisition (equal); Supervision (equal); Writing – original draft (supporting); Writing – review & editing (equal). **Mikel Sanz**: Conceptualization (lead); Funding acquisition (equal); Methodology (equal); Supervision (equal); Writing – review & editing (equal).

DATA AVAILABILITY

The data that support the findings of this study are available within the article and its supplementary material and from the corresponding author upon reasonable request.

REFERENCES

[1] M. Tavis and F. W. Cummings, "Exact solution for an *N*-molecule—Radiation-field Hamiltonian," Phys. Rev. **170**, 379 (1968).

[2] M. Aspelmeyer, T. J. Kippenberg, and F. Marquardt, "Cavity optomechanics," Rev. Mod. Phys. **86**, 1391 (2014).

[3] M. K. Schmidt, R. Esteban, A. González-Tudela, G. Giedke, and J. Aizpurua, "Quantum mechanical description of Raman scattering from molecules in plasmonic cavities," ACS Nano **10**, 6291 (2016).

[4] A. Blais, A. L. Grimsmo, S. M. Girvin, and A. Wallraff, "Circuit quantum electrodynamics," Rev. Mod. Phys. **93**, 025005 (2021).

[5] H. J. Kimble, "The quantum internet," Nature **453**, 1023 (2008).

[6] Y. Arakawa and M. J. Holmes, "Progress in quantum-dot single photon sources for quantum information technologies: A broad spectrum overview," Appl. Phys. Rev. **7**, 021309 (2020).

[7] J. Zhang and Y. Kivshar, "Quantum metaphotonics: Recent advances and perspective," APL Quantum **1**, 020902 (2024).

[8] W. J. Munro, K. Azuma, K. Tamaki, and K. Nemoto, "Inside quantum repeaters," IEEE J. Sel. Top. Quantum Electron. **21**, 78 (2015).

[9] K. Azuma, S. E. Economou, D. Elkouss, P. Hilaire, L. Jiang, H.-K. Lo, and I. Tzitrin, "Quantum repeaters: From quantum networks to the quantum internet," Rev. Mod. Phys. **95**, 045006 (2023).

[10] K. Heshami, D. G. England, P. C. Humphreys, P. J. Bustard, V. M. Acosta, J. Nunn, and B. J. Sussman, "Quantum memories: Emerging applications and recent advances," J. Mod. Opt. **63**, 2005 (2016).

[11] Y. Lei, F. Kimiaee Asadi, T. Zhong, A. Kuzmich, C. Simon, and M. Hosseini, "Quantum optical memory for entanglement distribution," Optica **10**, 1511 (2023).

[12] S. Wang, Z.-Q. Yin, D.-Y. He, W. Chen, R.-Q. Wang, P. Ye, Y. Zhou, G.-J. Fan-Yuan, F.-X. Wang, W. Chen *et al.*, "Twin-field quantum key distribution over 830-km fibre," Nat. Photonics **16**, 154 (2022).

[13] S. M. Girvin, "Circuit QED: Superconducting qubits coupled to microwave photons," in *Quantum Machines: Measurement and Control of Engineered Quantum Systems*, *Lecture Notes of the Les Houches Summer School*, edited by M. Devoret, B. Huard, R. Schoelkopf and L. F. Cugliandolo (Oxford University Press, Oxford, 2014), Vol. 96, pp. 113–256.

[14] X. Gu, A. F. Kockum, A. Miranowicz, Y. X. Liu, and F. Nori, "Microwave photonics with superconducting quantum circuits," Phys. Rep. **718–719**, 1 (2017).

[15] X. Li, J. Chen, P. Voss, J. Sharping, and P. Kumar, "All-fiber photon-pair source for quantum communications: Improved generation of correlated photons," Opt. Express **12**, 3737 (2004).

[16] A. G. Radnaev, Y. O. Dudin, R. Zhao, H. H. Jen, S. D. Jenkins, A. Kuzmich, and T. A. B. Kennedy, "A quantum memory with telecom-wavelength conversion," Nat. Phys. **6**, 894 (2010).

[17] N. Lauk, N. Sinclair, S. Barzanjeh, J. P. Covey, M. Saffman, M. Spiropulu, and C. Simon, "Perspectives on quantum transduction," Quantum Sci. Technol. **5**, 020501 (2020).

[18] D. Awschalom, K. K. Berggren, H. Bernien, S. Bhave, L. D. Carr, P. Davids, S. E. Economou, D. Englund, A. Faraon, M. Fejer *et al.*, "Development of quantum interconnects (QuICs) for next-generation information technologies," PRX Quantum **2**, 017002 (2021).

[19] A. H. Gnauck, R. M. Jopson, C. J. McKinstrie, J. C. Centanni, and S. Radic, "Demonstration of low-noise frequency conversion by Bragg scattering in a fiber," Opt. Express **14**, 8989 (2006).

[20] A. Gogyan and Y. Malakyan, "Entanglement-preserving frequency conversion in cold atoms," Phys. Rev. A **77**, 033822 (2008).

[21] H. J. McGuinness, M. G. Raymer, and C. J. McKinstrie, "Theory of quantum frequency translation of light in optical fiber: Application to interference of two photons of different color," Opt. Express **19**, 17876 (2011).

[22] S. Ramelow, A. Fedrizzi, A. Poppe, N. K. Langford, and A. Zeilinger, "Polarization-entanglement-conserving frequency conversion of photons," Phys. Rev. A **85**, 013845 (2012).

[23] A. S. Clark, S. Shahnia, M. J. Collins, C. Xiong, and B. J. Eggleton, "High-efficiency frequency conversion in the single-photon regime," Opt. Lett. **38**, 947 (2013).

[24] L. A. Williamson, Y.-H. Chen, and J. J. Longdell, "Magneto-optic modulator with unit quantum efficiency," Phys. Rev. Lett. **113**, 203601 (2014).

[25] P. S. Donvalkar, V. Venkataraman, S. Clemmen, K. Saha, and A. L. Gaeta, "Frequency translation via four-wave mixing Bragg scattering in Rb filled photonic bandgap fibers," Opt. Lett. **39**, 1557 (2014).

[26] S. Lefrancois, A. S. Clark, and B. J. Eggleton, "Optimizing optical Bragg scattering for single-photon frequency conversion," Phys. Rev. A **91**, 013837 (2015).

[27] B. A. Bell, J. He, C. Xiong, and B. J. Eggleton, "Frequency conversion in silicon in the single photon regime," Opt. Express **24**, 5235 (2016).

[28] L. Fan, C. L. Zou, M. Poot, R. Cheng, X. Guo, X. Han, and H. X. Tang, "Integrated optomechanical single-photon frequency shifter," Nat. Photonics **10**, 766 (2016).

[29] S. Clemmen, A. Farsi, S. Ramelow, and A. L. Gaeta, "All-optically tunable buffer for single photons," Opt. Lett. **43**, 2138 (2018).

[30] K. A. G. Bonsma-Fisher, P. J. Bustard, C. Parry, T. A. Wright, D. G. England, B. J. Sussman, and P. J. Mosley, "Ultratunable quantum frequency conversion in photonic crystal fiber," Phys. Rev. Lett. **129**, 203603 (2022).

[31] P. S. Russell, P. Hölzer, W. Chang, A. Abdolvand, and J. C. Travers, "Hollow-core photonic crystal fibres for gas-based nonlinear optics," Nat. Photonics **8**, 278 (2014).

[32] E. Numkam-Fokoua, S. Abokhamis Mousavi, G. T. Jasion, D. J. Richardson, and F. Poletti, "Loss in hollow-core optical fibers: Mechanisms, scaling rules, and limits," Adv. Opt. Photonics **15**, 1 (2023).

[33] A. V. Sokolov, "Giving entangled photons new colors," Science **376**, 575 (2022).

[34] R. Tyumenev, J. Hammer, N. Y. Joly, P. S. J. Russell, and D. Novoa, "Tunable and state-preserving frequency conversion of single photons in hydrogen," Science **376**, 621 (2022).

[35] A. Hamer, F. Vewinger, T. Peters, M. H. Frosz, and S. Stellmer, "Frequency conversion in a hydrogen-filled hollow-core fiber using continuous-wave fields," Opt. Lett. **49**, 6952 (2024).

[36] S. T. Bauerschmidt, D. Novoa, A. Abdolvand, and P. S. J. Russell, "Broadband-tunable LP_{01} mode frequency shifting by Raman coherence waves in a H_2-filled hollow-core photonic crystal fiber," Optica **2**, 536 (2015).

[37]M. A. Finger, T. S. Iskhakov, N. Y. Joly, M. V. Chekhova, and P. S. J. Russell, "Raman-free, noble-gas-filled photonic-crystal fiber source for ultrafast, very bright twin-beam squeezed vacuum," Phys. Rev. Lett. **115**, 143602 (2015).
[38]M. Antesberger, C. M. D. Richter, F. Poletti, R. Slavík, P. Petropoulos, H. Hübel, A. Trenti, P. Walther, and L. A. Rozema, "Distribution of telecom entangled photons through a 7.7 km antiresonant hollow-core fiber," Opt. Quantum **2**, 173 (2024).
[39]J. Q. Liang, M. Katsuragawa, F. L. Kien, and K. Hakuta, "Sideband generation using strongly driven Raman coherence in solid hydrogen," Phys. Rev. Lett. **85**, 2474 (2000).
[40]J. J. Weber, J. T. Green, and D. D. Yavuz, "17 THz continuous-wave optical modulator," Phys. Rev. A **85**, 013805 (2012).
[41]P. Hosseini, D. Novoa, A. Abdolvand, and P. S. J. Russell, "Enhanced control of transient Raman scattering using buffered hydrogen in hollow-core photonic crystal fibers," Phys. Rev. Lett. **119**, 253903 (2017).
[42]M. K. Mridha, D. Novoa, P. Hosseini, and P. S. J. Russell, "Thresholdless deep and vacuum ultraviolet Raman frequency conversion in hydrogen-filled photonic crystal fiber," Optica **6**, 731 (2019).
[43]M. G. Raymer, I. A. Walmsley, J. Mostowski, and B. Sobolewska, "Quantum theory of spatial and temporal coherence properties of stimulated Raman scattering," Phys. Rev. A **32**, 332 (1985).
[44]M. G. Raymer and I. A. Walmsley, "III the quantum coherence properties of stimulated Raman scattering," Prog. Opt. **28**, 181 (1990).
[45]A. A. Svidzinsky, X. Zhang, and M. O. Scully, "Quantum versus semiclassical description of light interaction with atomic ensembles: Revision of the Maxwell–Bloch equations and single-photon superradiance," Phys. Rev. A **92**, 013801 (2015).
[46]J. Wang, A. V. Sokolov, and G. S. Agarwal, "Quantum entanglement between signal and frequency-up-converted idler photons," Phys. Rev. A **108**, 063706 (2023).
[47]S. E. Harris and A. V. Sokolov, "Subfemtosecond pulse generation by molecular modulation," Phys. Rev. Lett. **81**, 2894 (1998).
[48]A. Nazarkin, G. Korn, M. Wittmann, and T. Elsaesser, "Generation of multiple phase-locked Stokes and anti-Stokes components in an impulsively excited Raman medium," Phys. Rev. Lett. **83**, 2560 (1999).
[49]A. Aghababaei, C. Biesek, F. Vewinger, and S. Stellmer, "Frequency conversion in pressurized hydrogen," Opt. Lett. **48**, 45 (2023).
[50]A. Hamer, S. M. Razavi Tabar, P. Yashwantrao, A. Aghababaei, F. Vewinger, and S. Stellmer, "Frequency conversion to the telecom O-band using pressurized hydrogen," Opt. Lett. **49**, 506 (2024).
[51]D. K. Veirs and G. M. Rosenblatt, "Raman line positions in molecular hydrogen: H_2, HD, HT, D_2, DT, and T_2," J. Mol. Spectrosc. **121**, 401 (1987).
[52]M. O. Scully and M. S. Zubairy, *Quantum Optics* (Cambridge University Press, Cambridge, 1997).
[53]T. K. Begzjav, Z. Yi, and J. S. Ben-Benjamin, "Effective Raman Hamiltonian revisited," Sci. Trans. Natl. Univ. Mong. Phys. **32**, 1 (2022).
[54]D. F. Walls, "Quantum theory of the Raman effect: II. Molecular coherence effects," Z. Phys. A **244**, 117 (1971).
[55]F. Benabid, J. C. Knight, G. Antonopoulos, and P. S. J. Russell, "Stimulated Raman scattering in hydrogen-filled hollow-core photonic crystal fiber," Science **298**, 399 (2002).
[56]F. T. Arecchi, E. Courtens, R. Gilmore, and H. Thomas, "Atomic coherent states in quantum optics," Phys. Rev. A **6**, 2211 (1972).
[57]Y. H. Chen and F. Wise, "Unified and vector theory of Raman scattering in gas-filled hollow-core fiber across temporal regimes," APL Photonics **9**, 030902 (2024).
[58]J. Tucker and D. F. Walls, "Quantum theory of parametric frequency conversion," Ann. Phys. **52**, 1 (1969).
[59]P. Kumar, "Quantum frequency conversion," Opt. Lett. **15**, 1476 (1990).
[60]W. K. Wootters, "Entanglement of formation of an arbitrary state of two qubits," Phys. Rev. Lett. **80**, 2245 (1998).
[61]S. Hill and W. K. Wootters, "Entanglement of a pair of quantum bits," Phys. Rev. Lett. **78**, 5022 (1997).
[62]Y.-F. Huang, X.-L. Niu, Y.-X. Gong, J. Li, L. Peng, C.-J. Zhang, Y.-S. Zhang, and G.-C. Guo, "Experimental measurement of lower and upper bounds of concurrence for mixed quantum states," Phys. Rev. A **79**, 052338 (2009).
[63]F. Mintert and A. Buchleitner, "Observable entanglement measure for mixed quantum states," Phys. Rev. Lett. **98**, 140505 (2007).
[64]C.-J. Zhang, Y.-X. Gong, Y.-S. Zhang, and G.-C. Guo, "Observable estimation of entanglement for arbitrary finite-dimensional mixed states," Phys. Rev. A **78**, 042308 (2008).
[65]R. L. Carman, F. Shimizu, C. S. Wang, and N. Bloembergen, "Theory of Stokes pulse shapes in transient stimulated Raman scattering," Phys. Rev. A **2**, 60 (1970).
[66]S. A. Akhmanov, Y. E. D'Yakov, and L. I. Pavlov, "Statistical phenomena in Raman scattering stimulated by a broad-band pump," Sov. Phys. JETP **39**, 249 (1974).
[67]M. G. Raymer, J. Mostowski, and J. L. Carlsten, "Theory of stimulated Raman scattering with broad-band lasers," Phys. Rev. A **19**, 2304 (1979).
[68]M. G. Raymer and J. Mostowski, "Stimulated Raman scattering: Unified treatment of spontaneous initiation and spatial propagation," Phys. Rev. A **24**, 1980 (1981).
[69]S. T. Bauerschmidt, D. Novoa, and P. S. J. Russell, "Dramatic Raman gain suppression in the vicinity of the zero dispersion point in a gas-filled hollow-core photonic crystal fiber," Phys. Rev. Lett. **115**, 243901 (2015).
[70]G. P. Agrawal, *Nonlinear Fiber Optics* (Academic Press, San Diego, 2007).